A 30-88 GHz Phase Shifter with Broadband 90° Hybrid- Marchand Balun Network and Common-base Buffer Achieving 1.34-3.1° RMS Phase Error in 90 nm SiGe

Zheng Liu, Emir Ali Karahan, Kaushik Sengupta
Princeton University, USA

***Abstract*— To enable a software-defined spectrally agile phased array operation across multiple bands from 30-100 GHz, we present a 30-88 GHz broadband IQ vector modulator phase shifter in 90 nm SiGe. This was enabled by 1) A single-end to differential quadrature phase generator consisting of a compact Marchand balun and 90°hybrid-based bandwidth extension network; 2) A common-base (CB) stage as the input buffer of the IQ VGA. Across the 58 GHz bandwidth, the maximum phase error of the 5-bit phase shifter is below half LSB resolution while achieving rms phase error of 1.34-3.1° and rms gain error of 0.19-0.48 dB. To the best of the authors' knowledge, this is the first phase shifter that covers from 5G FR2 to W band with a fractional bandwidth of 98.3% and demonstrates the best amplitude/phase error over one of the widest bandwidths.**

***Keywords*— Phase shifter, ultra-wideband, IQ vector modulator, common-base, 90° hybrid, Marchand balun, SiGe.**

I. Introduction

A frequency agile mmWave phased array front-end covering the evolving spectrum between 24-100 GHz for 5G beyond brings enormous advantages over conventional narrow band phased array solution in terms of multi-functionality, throughput, system size and cost. Achieving gain independent high accuracy phase control across broadband (>3:1 bandwidth) poses strong challenges on phase shifters design. Recent progress in broadband mmWave phase shifters above 24 GHz utilizes RF switches to demonstrate "reconfigurable multi-band" on either passive [1], [2], [3] or active [4] phase shifter core, suffering from limited phase control range and high RF switch loss. An "RF switch-less" broadband vector IQ modulator phase shifter using Quadrature All pass Filter (QAF) broadband quadrature phase generation has been explored [5], [6] but the network is very sensitive to the load (eg. transistor gate capacitance) which significantly degrades the bandwidth. Inductive loading and de-Q techniques[5], [6] mitigate the issue but the intrinsic loss due to resistance components in QAF is typically high (>10 dB loss in [5]). Moreover, the code-dependent input impedance of the active stage exacerbates the loading effect of QAF.

To enable a broadband IQ vector modulator across 30-88 GHz, we use a 90° hybrid and Marchand balun-based network for wideband single-ended to differential quadrature phase generation with accurate phase/amplitude response. For the IQ VGAs and analog adder, a differential Common-base (CB) buffer stage allows ideal broadband and code independent impedance loading to the quadrature phase generation network.

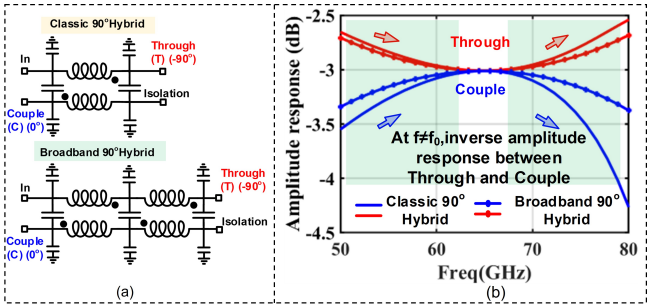

Fig. 1. (a) Transformer-based classic and broadband 90° hybrid; (b) The amplitude response of "Through" and "Couple" path.

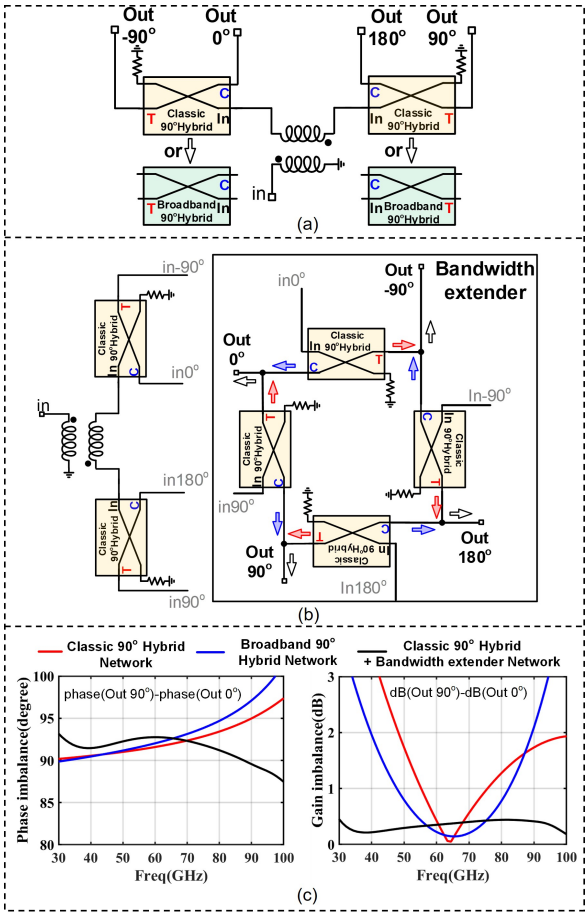

Fig. 2. Differential quadrature phase generation networks. (a) Balun with classic or broadband 90° hybrid; (b) Network of (a) with a 90° hybrid-based frequency extender; (c) Comparison of EM simulated phase/gain imbalance across 30-100GHz among three topologies.

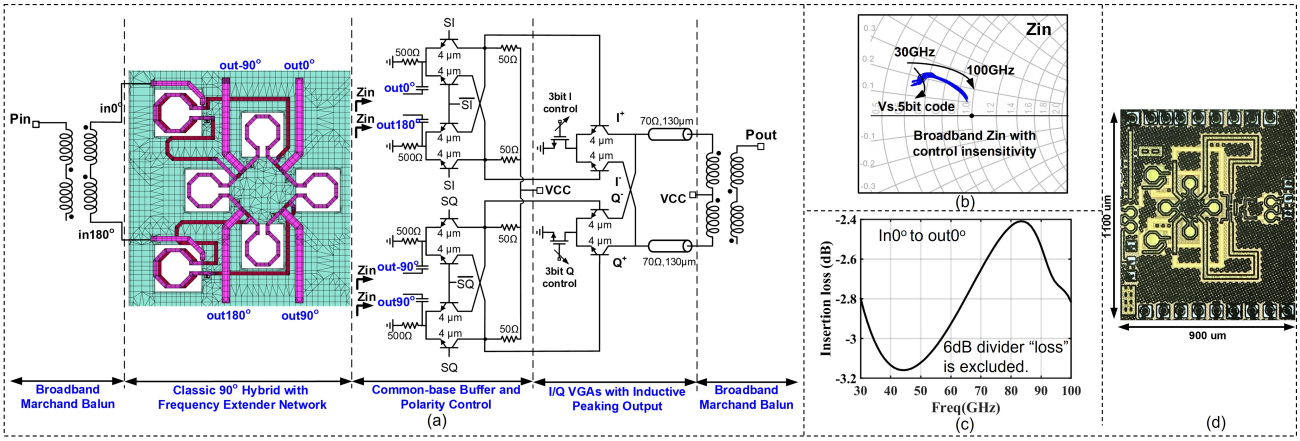

Fig. 3. (a) Circuit schematic; (b) Broadband matching and code insensitive input impedance of CB buffer; (c) Insertion loss of the EM simulated ultra-wideband input differential quadrature phase generation network across 30-100GHz; (d) Chip micrograph.

5-bit accuracy with maximum phase error smaller than half LSB is demonstrated across 98.3% bandwidth up to W band.

II. Ultra-Wideband Phase Shifter

A. Ultra-Wideband Differential Quadrature Phase Generation

For broadband quadrature phase generation, a compact transformer-based classic quadrature hybrid [7], [8] (Fig.1 (a)) can enable a 0.1° phase imbalance fractional bandwidth of 23% while a broadband quadrature hybrid in [9] (Fig. 1 (a)) enhances the phase imbalance bandwidth to 90.5%. However, the amplitude imbalance bandwidth for both hybrids still limits the bandwidth of a quadrature phase generation network. Fig. 1 (b) shows the amplitude versus frequency response of the 'through' and 'couple' path of both hybrids where a better amplitude imbalance can be seen for broadband hybrid, but a 0.5 dB amplitude imbalance bandwidth around 40% still cannot fulfill the need of ultra-wideband phase shifter application. A key observation is that the 'through' and 'couple' port has an inverse amplitude response away from the center frequency. To generate two differential quadrature phase signals feeding differential I/Q VGAs, a balun is used to feed its balanced output to two 90° hybrids (either classic or broadband) (Fig.2(a)). In this work, the two differential outputs of this network are fed to a bandwidth extender shown in Fig. 2(b). The bandwidth extender generates each output by combining two signals generated by 'through' and 'couple' path respectively. As an example, the 0° output can be generated by combining 1) the coupled output of a 0° input signal and 2) the 'through' output of a 90° input signal. Utilizing the property of the inverse amplitude response between 'through' and 'couple' paths, the gain compensation across frequency results in a more broadband amplitude response [8]. Fig.2 (c) compares the electromagnetically (EM) simulated phase and gain imbalance across frequency among the three networks, exhibiting a significant gain imbalance improvement using the bandwidth extender network (< 0.5 dB across 30-100 GHz). The bandwidth extender consists of four compact transformer-based classic quadrature hybrids,

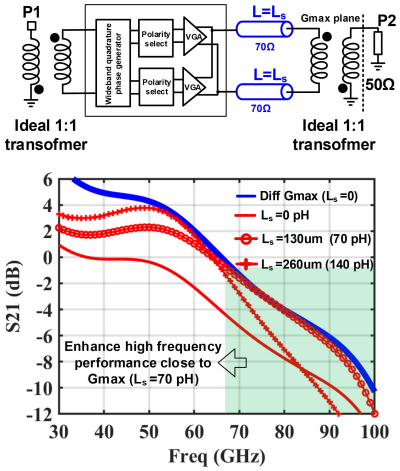

Fig. 4. Inductive peaking to enhance high frequency gain close to G_{max}.

therefore the whole network is relatively simple to build based on a single unit block. The EM simulated insertion loss of the whole quadrature generation network (without Marchand balun) is 2.4-3.1 dB across 30-100 GHz.

B. IQ VGAs with CB Buffer and Inductive Peaking

The conventional Gilbert cell VGAs [10] has a three-stack architecture which limits the headroom or power. More importantly, the gain control is done by varying the transistor bias current which causes parasitic capacitance variation, therefore the change of input impedance. Variations in the input impedance affect the quadrature generator network, resulting in additional gain and phase error [11]. To reduce this effect, this work implements a CB buffer embedded with phase quadrant control as the interface between quadrature generation and active VGA core. Shown in Fig. 3 (a), the four outputs from the quadrature generation network are fed to the emitter of the CB transistor for broadband matching. At the same time, the differential I/Q buffers allow the polarity change of the I/Q signals by controlling the base voltage of the CB transistors. Each output from quadrature

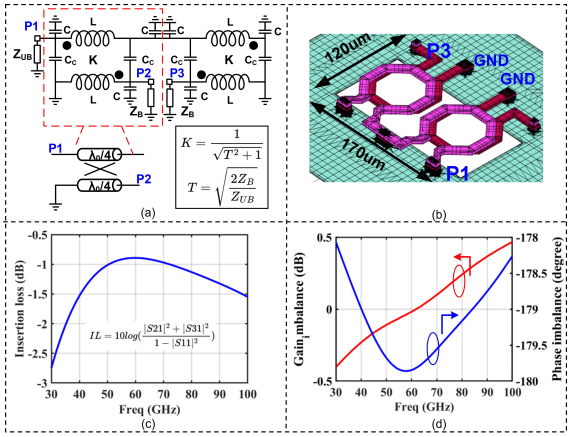

Fig. 5. Transformer based Marchand balun design;(a) Lumped model; (b) Layout; (c) Insertion loss; (d) Phase/gain imbalance across 30-100GHz.

network always sees one on-transistor and off-transistor across different polarity control, therefore offering a broadband code-independent input impedance Zin (Fig. 3 (b)). The output of the buffer is followed by I/Q differential VGAs and analog adder with 3-bit bias current control. Along with 2-bit polarity control in the first buffer stage, the phase shifter can work across all four quadrants with 5-bit control. Fig. 4 describes the inductive peaking technique at the output of the IQ VGAs, for bandwidth broadening across 30-100 GHz. We first extract the fully differential G_{max} (blue curve) of the phase shifter and a proper series high impedance Tline (130um Length) is added to enhance high frequency (>70 GHz) gain by 4 dB and to be close to G_{max}. The simulated differential gain of the phase shifter is about -6 to 4 dB across 30-88 GHz and the gain slope can be compensated by another high pass amplifier in the design of the full beamformer chain.

C. *Broadband Transformer Based Marchand Balun*

The phase shifter operates fully differential in the beamformer chain, but on-chip single-ended to differential conversion needs to be designed for evaluation performance. Transformer-based broadband Marchand balun is designed in this work. The layout is based on the lumped modeling shown in Fig. 5(a) where coupling factor K determines the balun impedance transformation ratio. The compact layout, insertion loss and balancing metrics are summarized in Fig. 5 (b) (c) and (d). Lower than 0.5 dB gain imbalance and lower than 2° phase imbalance over 30-100 GHz are exhibited.

III. Measurement Results

The prototype is implemented in 90 nm SiGe and chip photo is shown in Fig. 3 (d). It consumes 24 mW power under 2V supply. The phase/amplitude response is measured using Anritsu M4647B VNA with a frequency extender up to 110GHz. Even though the ultra-wideband quadrature generation network allows a frequency-independent code setting, a post-silicon frequency-dependent code optimization which can correct the potential quadrature phase mismatch due to process variation, allows a further performance

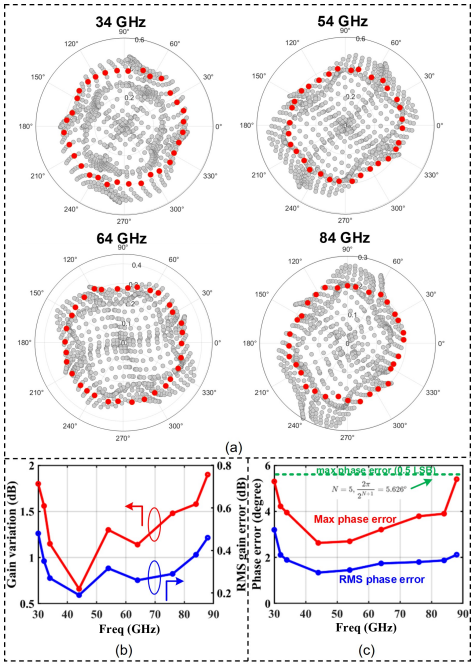

Fig. 6. (a) Measured amplitude/phase polar plot at 34,54,64 and 84GHz; (b) Measured gain variation and rms gain error vs. frequency; (c) Measured max phase error and rms phase error vs. frequency.

improvement in terms of phase error and gain variation across frequency. An optimization program is developed to rapidly synthesis the best code at user specified frequencies (for example at 34, 44, 54, 64, 74, 84 GHz and each code is applied within a 10 GHz bandwidth) to minimize the phase and gain variation. Fig. 6 (a) shows the measured amplitude/phase polar plot at 34, 54, 64 and 84GHz. Across 30-88 GHz, the gain variation across 32 codes is about 0.7-1.8 dB while the rms gain error is 0.19-0.48 dB (Fig. 6 (b)). The very low rms phase error of 1.34-3.1° and a maximum phase error of 2.63-5.4° are achieved across the 98.3% bandwidth. Maximum phase error lowering than half LSB (5.625°) demonstrates the 5-bit accuracy of this work.

Fig. 7 shows the measured broadband S21 and S11 across

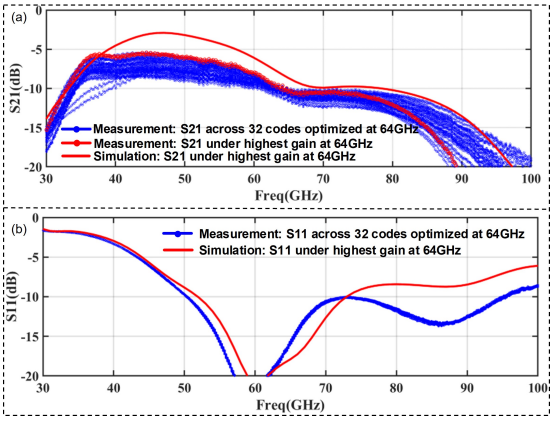

Fig. 7. (a) Measured vs. simulated S21 performance; (b) Measured vs. simulated S11.

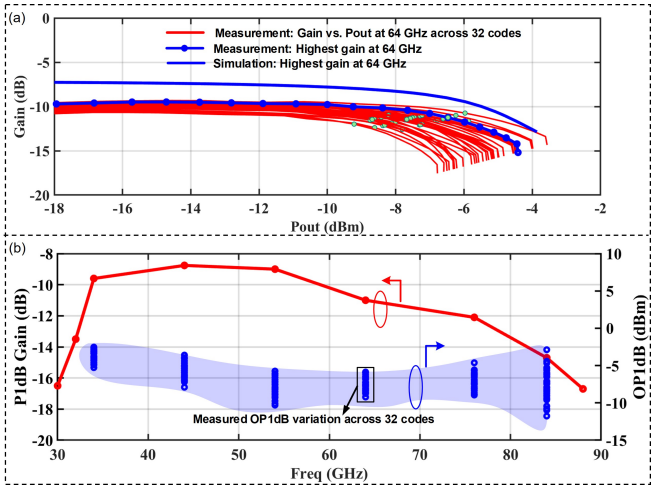

Fig. 8. (a) Measured vs. simulated CW performance at 64 GHz; (b) Measured Op1dB performance across frequency.

		Broadband Phase Shifters					E band and W band Phase shifters	
	This work	Alhamed JSSC 22′	Anjos TMTT 20′	Xiong TCAS 20′	Hossein CSICS 17′	Sah TMTT 13′	Yu TMTT 16′	Pepe JSSC 17′
Technology	90nm SiGe	90nm SiGe	250nm BiCMOS	90nm CMOS	45nm SOI	180nm BiCMOS	90nm CMOS	28nm SOI
Method	Frequency extended VS	QAF VS	Switchable passive	Switchable VS	Vector sum	Vector sum	Current reuse VS	Vector sum
0.5 LSB Error BW (GHz) *	30-88 (98.3%)	–	14-50 (112.5%)	–	–	–	–	–
Measurement BW (GHz) **	30-100 (107.6%)	16-52 (105.8%)	14-50 (112.5%)	24-41 (52.3%)	58-84 (37%)	15-35 (87%)	57-64 (11.5%)	78-93 (16.3%)
Phase range	360°	360°	180°	360°	360°	360°	360°	360°
Phase resolution (bit)	5	5	2	5	5	4	4	4
Gain (avg.) (dB)	-7.8 – -15.7 (4 – -6 w/o balun)	–	-5 – -16	-4.5 – -7	-6 – -9	5– -13.5	1.1	2.3
Max phase error (°)	2.63-5.4	–	5.8-22.5	–	–	–	4.5-15	–
RMS gain error (dB)	0.19-0.48	<1.7	<0.94	0.1-0.6	0.8-1.1	1- 2.2	0.75-1.6	1.68-2
RMS phase error (°)	1.34-3.1	<5.6	<9.7	2-5.1	2.7-10.1	4.2-13	2.3-7.6	9.4-11.9
Output P1dB (avg.) (dBm)	-5 – -2.5	–	–	>-10.7	-1@ 70GHz	-1.25 – -19.8	-8.7 @ 60GHz	-4.7@ 87GHz
Noise Figure(dB)	17 @ 60G	–	–	–	–	–	11@60G	12@89G
Power (mW)	24	26	0	17.6	17	25.2	19.8	21.6
Chip area (mm^2)	0.99(with pads)	–	0.48(w/o pads)	0.34(w/o pads)	0.11(w/o pads)	0.19 (w/o pads)	0.61(with pads)	0.12 (w/o pads)

Fig. 9. Comparison with state of the art mmWave broadband phase shifters.

32 codes and its correlation with simulation. An acceptable correlation is seen. Considering the fully differential gain of the phase shifter is 4 to -6 dB across 30-88 GHz, the measured gain at the lower band edge is due to the imperfect input matching of the Marchand balun. Fig. 8 (a) shows the measured gain vs. output power across 32 codes at 64 GHz, along with a good large signal correlation between simulation. The average OP1dB is from -2.5 to -5 dBm across 34-84 GHz. Compared with the state of the art mmWave broadband phase shifters (Fig. 9), this work demonstrates the best amplitude/phase errors over one of the widest bandwidths.

IV. Conclusion

We presents the first ultra-wideband phase shifter covering 30-88 GHz in 90 nm SiGe technology. Across the 58 GHz bandwidth, the maximum phase error of the 5 bit phase shifter is below half LSB resolution while achieving low rms phase error of 1.34-3.1° and low rms gain error of 0.19-0.48 dB, the lowest errors for one of the widest bandwidths reported. This work covers all bands from 5G FR2 to W band, and can open door to a frequency agile, multi-standard array front-end with beamforming capability across 24-100 GHz.

Acknowledgment

The authors would like to acknowledge Defense Advanced Research Program Agency (DARPA) YFA program and Dr. Tim Hancock, Army Research Office and Dr. Joe Qiu for funding support. The authors also acknowledge GlobalFoundries for fabrication support, and all members of IMRL for technical discussions.

References

[1] E. V. P. Anjos, D. M. M.-P. Schreurs, G. A. E. Vandenbosch, and M. Geurts, "A 14–50-ghz phase shifter with all-pass networks for 5g mobile applications," *IEEE Transactions on Microwave Theory and Techniques*, vol. 68, no. 2, pp. 762–774, 2020.

[2] X.-L. Huang, L. Zhou, Y. Yuan, L.-F. Qiu, and J.-F. Mao, "Quintuple-mode w-band packaged filter based on a modified quarter-mode substrate-integrated waveguide cavity," *IEEE Transactions on Components, Packaging and Manufacturing Technology*, vol. 9, no. 11, pp. 2237–2247, 2019.

[3] J.-T. Lim, S. Choi, E.-G. Lee, H.-W. Choi, J.-H. Song, S.-H. Kim, and C.-Y. Kim, "25–40 ghz 180° reflective-type phase shifter using 65-nm cmos technology," in *2019 49th European Microwave Conference (EuMC)*, 2019, pp. 480–483.

[4] Y. Xiong, X. Zeng, and J. Li, "A frequency-reconfigurable cmos active phase shifter for 5g mm-wave applications," *IEEE Transactions on Circuits and Systems II: Express Briefs*, vol. 67, no. 10, pp. 1824–1828, 2020.

[5] A. Alhamed, G. Gültepe, and G. M. Rebeiz, "A multi-band 16–52-ghz transmit phased array employing 4 × 1 beamforming ic with 14–15.4-dbm psat for 5g nr fr2 operation," *IEEE Journal of Solid-State Circuits*, vol. 57, no. 5, pp. 1280–1290, 2022.

[6] S. P. Sah, X. Yu, and D. Heo, "Design and analysis of a wideband 15–35-ghz quadrature phase shifter with inductive loading," *IEEE Transactions on Microwave Theory and Techniques*, vol. 61, no. 8, pp. 3024–3033, 2013.

[7] R. Frye, S. Kapur, and R. Melville, "A 2-ghz quadrature hybrid implemented in cmos technology," *IEEE Journal of Solid-State Circuits*, vol. 38, no. 3, pp. 550–555, 2003.

[8] T.-W. Li, J. S. Park, and H. Wang, "A 2–24-ghz 360° full-span differential vector modulator phase rotator with transformer-based poly-phase quadrature network," *IEEE Transactions on Very Large Scale Integration (VLSI) Systems*, vol. 28, no. 12, pp. 2623–2635, 2020.

[9] Z. Liu and K. Sengupta, "A 44–64-ghz mmwave broadband linear doherty pa in silicon with quadrature hybrid combiner and non-foster impedance tuner," *IEEE Journal of Solid-State Circuits*, vol. 57, no. 8, pp. 2320–2335, 2022.

[10] K.-J. Koh and G. M. Rebeiz, "0.13-μm cmos phase shifters for x-, ku-, and k-band phased arrays," *IEEE Journal of Solid-State Circuits*, vol. 42, no. 11, pp. 2535–2546, 2007.

[11] G. H. Park, C. W. Byeon, and C. S. Park, "A 60-ghz low-power active phase shifter with impedance-invariant vector modulation in 65-nm cmos," *IEEE Transactions on Microwave Theory and Techniques*, vol. 68, no. 12, pp. 5395–5407, 2020.